

# Sub 6 GHz Smartphone Antenna with Dual-Band Monopole Resonators for 5G Communications

Haleh Jahanbakhsh Basherlou<sup>1</sup>, Naser Ojaroudi Parchin<sup>1</sup>, Mohammad Alibakhshikenari<sup>2</sup>, Chan Hwang See<sup>1</sup>

<sup>1</sup> School of Computing, Engineering and the Built Environment, Edinburgh Napier University, Edinburgh, UK

<sup>2</sup> Department of Signal Theory and Communications, Universidad Carlos III de Madrid, 28911 Leganés, Madrid, Spain

[haleh.jahanbakhshbasherlou@napier.ac.uk](mailto:haleh.jahanbakhshbasherlou@napier.ac.uk), [n.ojaroudiparchin@napier.ac.uk](mailto:n.ojaroudiparchin@napier.ac.uk), [mohammad.alibakhshikenari@uc3m.es](mailto:mohammad.alibakhshikenari@uc3m.es), [c.see@napier.ac.uk](mailto:c.see@napier.ac.uk)

**Abstract**— This study represents the schematic and fundamental features of a new MIMO antenna with low-profile elements and suitable characteristics for future cellular communications. Two rows of low-profile hook-shaped ring-monopole antennas with discrete-fed topology are mounted on opposite sides of the board, forming an 8×8 MIMO network. On the same layer as the ground plane, the elements of the suggested design were etched and provided a dual-band function operating at 3.5 and 5.6 GHz of the sub-6 GHz cellular spectrum. The board layout allocates a limited space for the intended array. Due to the resonators' arrangement, the proposed design can function as dual high-gain beam-steerable phased arrays. In summary, the planned MIMO array is capable of delivering optimal performance, meeting the requirements for future 5G portable devices like smartphones and tablets.

**Keywords**— Smartphone antenna, 5G, cellular communications, handheld devices, MIMO, sub 6 GHz applications.

## I. INTRODUCTION

The current 4G wireless systems lack the necessary high data rates for future mobile networks, prompting the evolution to 5th generation (5G) technology that offers enhanced services to meet these challenges [1-4]. Wireless service providers are grappling with unprecedented challenges due to global bandwidth constraints arising from the surge in mobile data usage and widespread smartphone adoption [5].

To address these issues, future 5G networks incorporate Multiple Input Multiple Output (MIMO) systems, combining multiple inputs and outputs to achieve high transmission speeds, data rates, and throughput [6-7]. MIMO technology enables increased data rates, capacity, and coverage by mitigating multipath fading and minimizing coupling among antenna elements [8-10]. In the realm of mobile and cellular communications, microstrip and printed antennas are widely used due to their compact sizes and simple structures, enhancing their appeal [11-15]. However, optimizing the performance of MIMO arrays in cellular networks poses significant challenges that need careful consideration and resolution [16-19]. Among microstrip antennas, the simplicity, efficiency, and adaptability of monopole antennas make them indispensable components in the realization of high-performance MIMO systems [20].

This study introduces an innovative eight-element array with a compact configuration. The design covers the

frequencies of 3.3-3.7 GHz and 5.4-6 GHz, addressing the sub-6 GHz 5G cellular communication bands separately. The design approach is streamlined, employing a discrete feeding technique within a single layer of monopole-loop antenna elements. This MIMO array design achieves commendable results. While numerous studies explore eight-element MIMO antenna designs, this paper's focus lies in developing a system with strong MIMO characteristics while simplifying both the design and manufacturing processes. The characteristics of the proposed design were analyzed using CST 2020 [21]. The subsequent sections provide detailed schematics, fundamental properties of the proposed antenna system, and the study's conclusions.

## II. CONFIGURATION

A perspective top view of the proposed MIMO design can be seen in Figure 1. It is apparent from the diagram that the multi-feed antenna contains eight monopole-loop radiators deployed at different PCB sides. The ground plane and elements are etched at the same time. Table I outlines the specific parameter values used in this study.

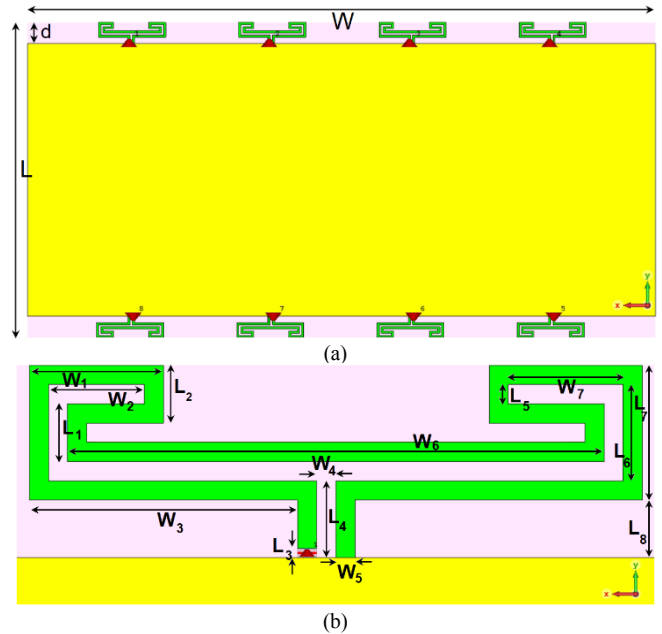


Fig. 1. (a) The MIMO antenna layout and its (b) single-element schematic.

TABLE I PARAMETER VALUES IN MILLIMETER (MM)

Parameter	W	L	W <sub>1</sub>	L <sub>1</sub>	W <sub>2</sub>	L <sub>2</sub>
Value (mm)	150	75	3.5	1.5	2.5	1.5
Parameter	W <sub>3</sub>	L <sub>3</sub>	W <sub>4</sub>	L <sub>4</sub>	W <sub>5</sub>	L <sub>5</sub>
Value (mm)	7	0.25	0.5	2	0.5	0.5
Parameter	W <sub>6</sub>	L <sub>6</sub>	W <sub>7</sub>	L <sub>7</sub>	L <sub>8</sub>	d
Value (mm)	14	2.5	3	3.5	1.5	5

### III. THE ESSENTIAL PROPERTIES

Figure 2 displays the S-parameters for the array design, illustrating key characteristics of the MIMO array's frequency responses, such as  $S_{11}$  (indicating reflection coefficient and impedance bandwidth) and  $S_{mn}$  (representing transmission coefficient). The findings reveal that, at a -10 dB threshold, the antenna functions effectively within two distinct frequency bands: 3.3-3.7 GHz and 5.4-6 GHz, with the possibility of exceeding these values at a -6 dB level. Furthermore, the designed elements exhibit favorable mutual couplings, measuring less than -11 dB.

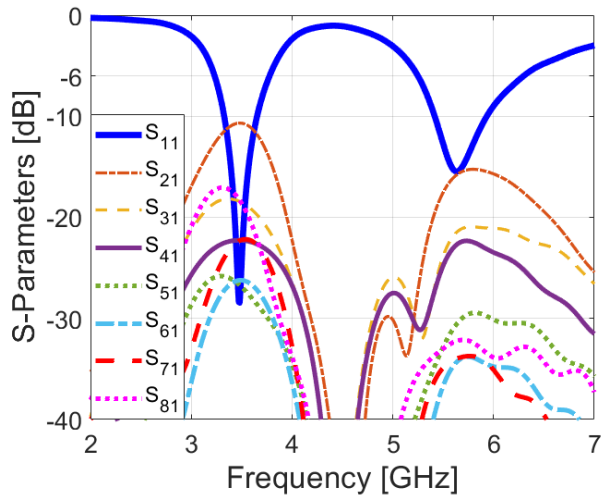


Fig. 2. The S-parameter results of the array.

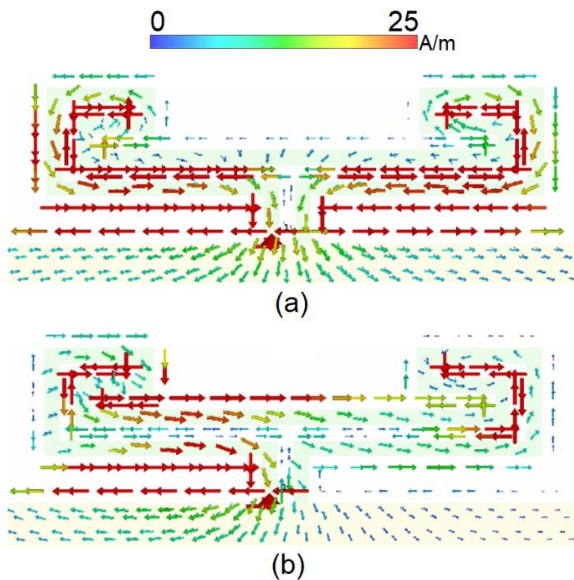


Fig. 3. Current densities at (a) 3.5 and (b) 5.6 GHz.

The surface currents of the designed hook-shaped ring-monopole element at its resonances of 3.5 and 5.6 GHz have been depicted in Fig. 3. The influence of internal and external dimensions, as well as varied sides of the proposed resonator, on resonance generation and the enhancement of antenna impedance bandwidth is evident [22-24]. Figure 3(a) illustrates this effect, where the external length of the resonator exhibiting high current densities corresponds to the lower frequency band, and conversely, to the higher frequency band.

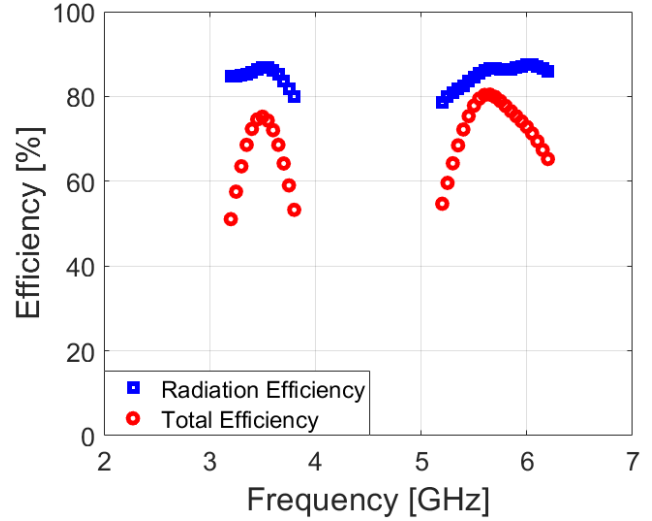


Fig. 4. Simulated radiation/total efficiencies.

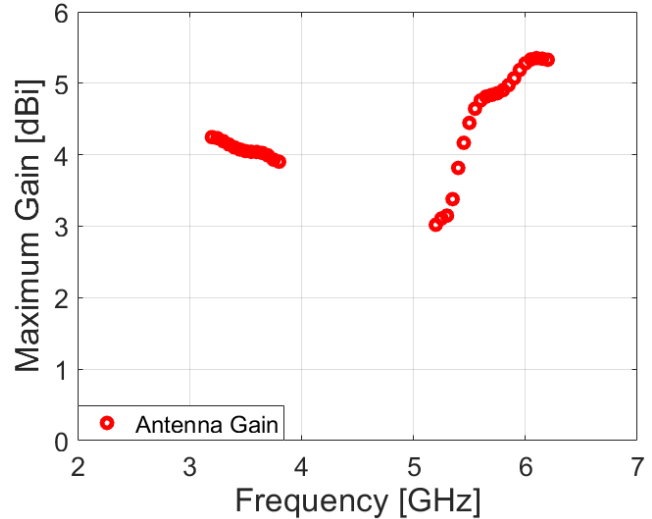


Fig. 5. Maximum gain results of the antenna.

As observed in Fig. 4, the suggested elements offers sufficient efficiencies. The radiation efficiency function is higher than 80% as represented. Furthermore, Fig. 4 also indicates that more than 50% total efficiencies can be achieved at both operational bandwidths. The maximum gain characteristics of the proposed antenna at its operation band is plotted in Fig. 5. It can be observed that more than 4 dBi gain is obtained over the first operation band. While, as shown, for the second operation, the antenna gain level varies from 3 to more than 5.3 dBi.

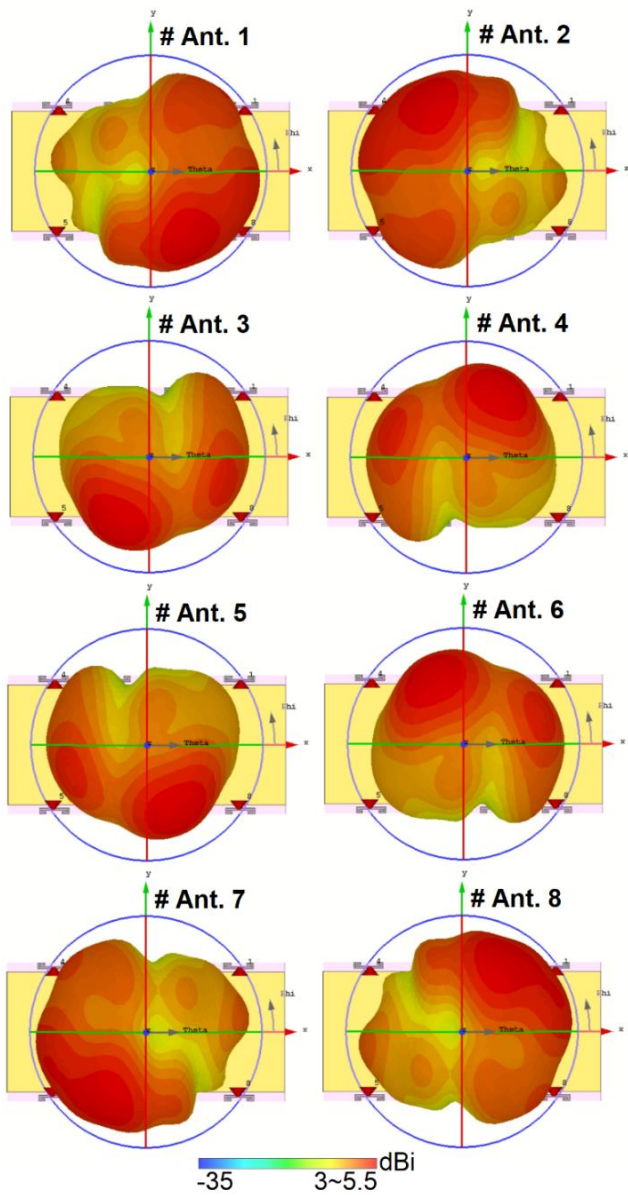


Fig. 6. Radiations at 3.5 GHz.

Figures 6 and 7 provide 3D visualizations of the radiated field at the resonating operational frequencies (3.5 and 5.6 GHz) for the elements within the suggested MIMO configuration, confirming the precisely defined radiation patterns of the antenna elements at these specific frequencies. These figures depict highly satisfactory radiations, ensuring consistent performance and adequate gain levels across the mainboard. These results validate the antenna's ability to offer diverse coverage while maintaining stable and sufficient signal strengths, as indicated in the existing literature [25-27].

To optimize gain and regulate radiation patterns, the design can be organized to create two  $1 \times 4$  beam-steerable arrays. Figure 8 assesses the primary radiation beam of one sub-array at its second resonance frequency, 5.6 GHz. The  $1 \times 4$  subarray has demonstrated its ability to produce high-gain radiation beams, enabling wide beam steering capabilities, as supported by previous research [29-30]. Similar performance

can be anticipated for the first resonance frequency, suggesting the consistent and reliable functionality of the design across different operational frequencies.

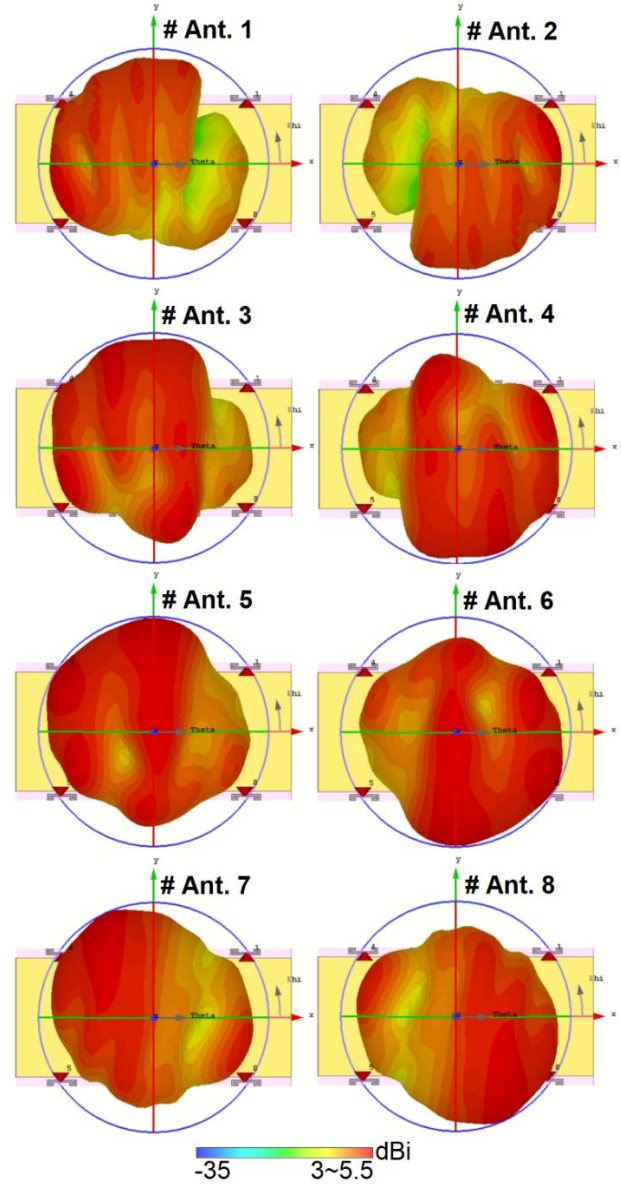


Fig. 7. Radiations at 5.6 GHz.

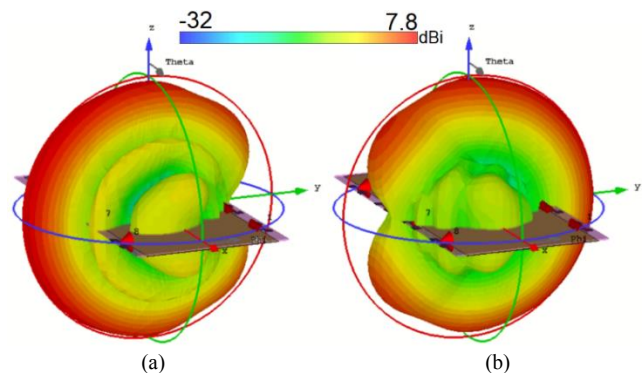


Fig. 8. Side-view radiations for the  $1 \times 4$  subarrays main scanning angle for the  $1 \times 4$  sub-arrays placed at different sides of the mainboard.

#### IV. CONCLUSION

This paper describes a MIMO smartphone antenna array with low-profile hook-shaped ring-monopoles and dual-operational bandwidth for 5G handheld devices and cellular IoT communications. Based on the schematic provided, the smartphone board features eight compact printed loop resonators on each side, designed to function effectively at both 3.5 and 5.6 GHz frequencies. The array was examined for a number of properties and satisfactory results were observed.

#### ACKNOWLEDGMENT

Dr. Mohammad Alibakhshikenari acknowledges support from the CONEX-Plus programme funded by Universidad Carlos III de Madrid and the European Union's Horizon 2020 research and innovation programme under the Marie Skłodowska-Curie grant agreement No. 801538.

#### REFERENCES

- [1] Y. Wang, *et al.*, "5G mobile: Spectrum broadening to higher-frequency bands to support high data rates," *IEEE Vehicular Technology Magazine*, vol. 9, pp. 39-46, 2014.
- [2] N. O. Parchin, R. A. Abdalhameed "A compact Vivaldi antenna array for 5G channel sounding applications," *EuCAP 2018*, 9-13 April 2018, London, UK.
- [3] M. Jensen, J. Wallace, "A review of antennas and propagation for MIMO wireless communications", *IEEE Trans. Antennas Propag.*, vol. 52, 2810-2824, 2004.
- [4] N. Ojaroudi, N. Ghadimi, "Design of CPW-Fed slot antenna for MIMO system applications," *Microw. Opt. Technol. Lett.*, vol. 56, pp. 1278-1281, 2014.
- [5] Y. Al-Yasir, *et al.*, "Green and Highly Efficient MIMO Transceiver System for 5G Heterogenous Networks," *IEEE Trans. Green Commun. Netw.* 2022.
- [6] N. Ojaroudiparchin, *et al.*, "Wide-scan phased array antenna fed by coax-to-microstriplines for 5G cell phones," *MIKON*, Poland, 2016.
- [7] J. Mazloun, *et al.*, "Compact triple-band S-shaped monopole diversity antenna for MIMO applications," *Applied Computational Electromagnetics Society (ACES) Journal*, vol. 28, pp. 975-980, 2015.
- [8] N. O. Parchin *et al.*, "Four-Element/Eight-Port MIMO Antenna System With Diversity and Desirable Radiation for Sub 6 GHz Modern 5G Smartphones," *IEEE Access*, vol. 10, pp. 133037-133051, 2022.
- [9] M. Abdullah, *et al.*, "Eight-element antenna array at 3.5GHz for MIMO wireless application," *PIER C*, vol. 78, pp. 209-217, 2017.
- [10] X.-T. Yuan, Z. Chen, T. Gu and T. Yuan, "A wideband PIFA-pair-based MIMO antenna for 5G smartphones," *IEEE Antennas and Wireless Propagation Letters*, vol. 20, no. 3, pp. 371-375, 2021.
- [11] A. Ullah, *et al.*, "Coplanar waveguide antenna with the defected ground structure for 5G millimeter-wave communications," *IEEE MENACOMM*, 19-21 Nov. 2019, Manama, Bahrain.
- [12] L. Wang, *et al.*, "Compact UWB MIMO antenna With high isolation using fence-type decoupling structure," *IEEE Antennas and Wireless Propagation Letters*, vol. 8, pp.1641 - 1645, 2019.
- [13] W. S. Chen, Y. C. Lai, and C. Y. D. Sim, "MIMO dongle antenna design for next generation mobile communication system," *IEEE International Conference on Computational Electromagnetics (ICCEM)*, 2017, pp. 320-322, vol. 8, pp.1641 - 1645, 2019.
- [14] M. Abdullah *et al.*, "Future Smartphone: MIMO Antenna System for 5G Mobile Terminals," in *IEEE Access*, vol. 9, pp. 91593-91603, 2021.
- [15] C. Shi, and Y. Sun, "Wideband Six-Port 5G MIMO Mobile Phone Antenna," *ICMMT*, pp. 1-3, 2021
- [16] Y. S. Faouri, *et al.*, "A Novel Meander Bowtie-Shaped Antenna with Multi-Resonant and Rejection Bands for Modern 5G Communications," *Electronics*, vol. 11, no. 5, p. 821, Mar. 2022.
- [17] N. Ojaroudi, "Design of microstrip antenna for 2.4/5.8 GHz RFID applications," *German Microwave Conference, GeMic 2014*, RWTH Aachen University, Germany, March 10-12, 2014.
- [18] N. Ojaroudi, M. Ojaroudi, and Sh. Amiri, "Enhanced bandwidth of small square monopole antenna by using inverted U-shaped slot and conductor-backed plane," *ACES Journal*, vol. 27, no. 8, pp. 685-690, 2012.
- [19] Y. I. A. Al-Yasir, *et al.*, "New Pattern Reconfigurable Circular Disk Antenna Using Two PIN Diodes for WiMax/WiFi (IEEE 802.11a) Applications," *SMACD*, Lausanne, Switzerland, 2019.
- [20] N. Ojaroudi, "Application of protruded strip resonators to design an UWB slot antenna with WLAN band-notched characteristic," *PIER C*, vol. 47, 111-117, 2014.
- [21] *CST Microwave Studio*, ver. 2020, CST, MA, USA, 2020.
- [22] N. Ojaroudi, and N. Ghadimi, "Dual-band CPW-fed slot antenna for LTE and WiBro applications," *Microw. Opt. Technol. Lett.*, vol. 56, pp. 1013-1015, 2014.
- [23] N. O. Parchin, "Low-profile air-filled antenna for next generation wireless systems," *Wireless Personal Communications*, vol. 97, pp. 3293-3300, 2017.
- [24] S. Ahmad *et al.*, "A Jug-Shaped CPW-Fed Ultra-Wideband Printed Monopole Antenna for Wireless Communications Networks," *Applied Sciences*, vol. 12, no. 2, p. 821, Jan. 2022.
- [25] B. H., Siahkal-Mahalle, *et al.*, "A new design of small square monopole antenna with enhanced bandwidth by using cross-shaped slot and conductor-backed plane," *Microw. Opt. Technol. Lett.*, vol. 54, 2656-2659, 2012.
- [26] M. S. Sharawi, "Advancements in MIMO antenna systems," Developments in antenna analysis and synthesis. Chapter-4. IET, 2018.
- [27] N. Ojaroudi, *et al.*, "Quad-Band Planar InvertedF Antenna (PIFA) for Wireless Communication Systems," *PIER Letters*, vol. 45, pp. 51-56, 2014.
- [28] N. O. Parchin, *et al.*, "Dual-Band Phased Array 5G Mobile-Phone Antenna with Switchable and Hemispherical Beam Pattern Coverage for MIMO-Diversity Communications", *ACES Journal*, vol. 36, no. 12, pp. 1602-1609, 2022.
- [29] M. E. Munir *et al.*, "A New mm-Wave Antenna Array with Wideband Characteristics for Next Generation Communication Systems," *Electronics*, vol. 11, no. 10, p. 1560, May 2022.
- [30] W. Hong *et al.*, "Multibeam antenna technologies for 5G wireless communications," *IEEE Trans. Antennas Propag.*, vol. 65, no. 12, pp. 6231-6249, 2017.